VARIATION IN Mn/Fe SYSTEMATICS IN PYROXENE FROM THE MOON: THE EFFECTS OF CONTRASTING Ti AND Al ACTIVITIES.
J. J. Papike, S. B. Simon, and C. K. Shearer. Institute of Meteoritics, Department of Earth and Planetary Sciences, University of New Mexico, Albuquerque, New Mexico 87131, U.S.A. (sbs8@unm.edu).

Introduction: Papike et al. [1] introduced a technique where the Mn/Fe ratios of olivine or pyroxene and the anorthite content of plagioclase provided a tool to identify the planetary parentage of newly discovered meteorites. A recent paper [2] refined this technique, focusing on the angrite meteorites, and a new, robust determinative curve was obtained. On a plot of Mn vs. Fe cations per formula unit for pyroxene from basalts, the slopes of the data trends decrease in the sequence Vesta, Mars, Earth, and Moon. Analyses of angrite pyroxenes are not directly comparable to those from the other bodies because in angrite pyroxenes the M2 sites are completely filled by Ca [e.g., 3] and therefore have different substitution systematics. Despite the fact that with enough high-quality electron microprobe data for olivine, pyroxene, and plagioclase we find an overarching fingerprint of planetary parentage, in any individual suite there is significant scatter along the average trend line. The purpose of this paper is to explore the dispersion of Mn/Fe ratios of pyroxene in lunar basalts and to illustrate the effect of crystallization sequence upon this parameter.

Lunar mare basalts are divided into three main types: high-Ti (from Apollo 11 and 17 landing sites); low-Ti (mainly from the Apollo 12 and 15 landing sites); and very-low-Ti basalts (VLT; from the Soviet Luna 24 (L-24) mission and from the Apollo 17 (A-17) drill core). All of the Apollo samples were collected within or immediately adjacent to the Procellarum KREEP Terrane (PKT; [4]), whereas the L-24 basalts represent melts derived from outside this terrane. Most of the analysis of lunar samples indicates a fairly limited range of oxygen fugacity, generally close to IW-1 (e.g., [5]). Thus, Ti is mainly in the 4+ oxidation state [6]. Rather than wide ranges in fO_2 or analytical error, the variability of Mn/Fe ratio in lunar basalt pyroxene is directly or indirectly dependent upon Ti concentrations in their mantle sources, as shown below.

There are many possible coupled substitution mechanisms in pyroxene, and these can be summarized using an equation assuming stoichiometric formulae (where coefficients indicate the magnitude of the excess/deficiency, such that, for example, $^{VI}Al^{3+}$ is equivalent to a +1 charge excess, while $2^{VI}Ti^{4+}$ indicates that for every Ti^{4+} substitution, there is a charge excess of +2). For lunar pyroxene, the equation expressing this completely is: Excesses: $^{VI}Al^{3+} + ^{VI}Fe^{3+} + ^{VI}Cr^{3+} + ^{VI}V^{3+} + ^{VI}Ti^{3+} + 2^{VI}Ti^{4+} =$ Deficiencies: $^{IV}Al^{3+} + ^{M2}Na^+$. In lunar pyroxenes, the Fe^{3+}, V^{3+} and Na components are very small. Coupled substitutions are required to incorporate trivalent cations and Ti^{4+} into the pyroxene crystal structure because they replace divalent Mg and Fe in the M1 site [7], thus creating an excess charge of +1 or +2, respectively. Crystal charge balance must be maintained, and and balancing of charge excesses can be accomplished by simultaneously substituting: 1) one Al cation into the tetrahedral site for Si; or 2) one Na cation into the M2 site for Ca, per unit of excess charge. Although pyroxenes from the three mare basalt groups exhibit a range of Mn/Fe ratios, the positioning of an individual point on a plot of Mn vs. Fe cations does not follow a simple sweep of Mn/Fe slope dependent only on Ti content. This is because, although $Ti^{4+}(M1) - 2Al$ (tet.) exchange is very important, it is not the only coupled substitution in play. The second most important is Al (M1) – Al (tet.). Therefore, the competing effects of variable Al vs. Ti content of pyroxene can change the positioning of an individual point. Substitution of Ti into pyroxene leads to increases in the Mn/Fe ratios because Ti^{4+} preferentially replaces Fe relative to Mn because its ionic radius is closer to that of Fe than Mn.

Methods: Data for pyroxene from high-Ti, low-Ti, and L-24 VLT basalts were taken from the literature [8-11]. The L-24 data were included in this study to examine the potential variability in mantle Mn/Fe outside of the PKT. The A-17 VLTs considered here are those studied by [12]. New analyses of pyroxene in these VLT samples were obtained with a JEOL 8200 fully automated electron microprobe at the University of New Mexico, operated at 15 kV. Counting times on peaks ranged from 10 to 30 s; background count times equaled the peak counting times for each analysis. Pure oxide, synthetic glass, and natural mineral standards were used. Average relative errors are ~6% for Ti and Mn, 2% for Al, and 0.5% for Fe. Fits to the data, both linear and polynomial, were generated by curve-fitting algorithms built into the KaleidaGraph v4.5 plotting software program. The polynomial fits are intended to be illustrative rather than a rigorous fit to the data.

Results: Individual analyses are plotted in Fig. 1a; polynomial fits are shown in Fig.1b; and linear fits in Fig. 1c. Although a single linear slope for lunar pyroxene analyses has been previously reported (e.g., [13]), in detail all four data sets have sinusoidal trends with positive trajectories (Fig. 1).

The high-Ti (HT) basalt data have a sharp increase in Mn content at low Fe#, a result of rapid, early incor-

poration of Ti into the pyroxene M1 site and consequent displacement of Fe, leading to increasing Mn/Fe ratios. This near-vertical trajectory continues until the Ti-oxides stop crystallizing. Next is a segment (Fe# from ~0.5-0.9) with a shallower slope. This is after plagioclase crystallizes. The inflection before (at lower Fe#) the flattened part of the trajectory occurs when plagioclase comes onto the liquidus and competes with pyroxene for Al, causing sharp drops in both Ti and Al contents in pyroxene. The last upturn involves a second increase of Ti activity in the melt, which enters the late-stage pyroxene and again displaces Fe, causing an increased Mn/Fe ratio and resulting in the crystallization of late-stage ilmenite and Ti-rich spinel.

As observed for the high-Ti pyroxene, a sinusoidal pattern with three main segments is observed for low-Ti basalt pyroxene on a plot of Mn cations against Fe# (Fig. 1a,b). The first segment reflects co-crystallization of olivine and pyroxene, with pyroxene incorporating Ti and Al in a ratio of ~¼ and Mn increasing sharply over a narrow range of Fe#. The second is a flattening when plagioclase comes onto the liquidus. The contents of Al and Ti cations are not as strongly correlated in the low-Ti basalts as they are in the high-Ti basalts because, with the lower initial Ti/Al in the parental melts of the former, two substitutional couples are involved. The first is, as above, Ti^{4+}(M1)- $2Al^{3+}$(Tet site, tetrahedral). The second is Al^{3+}(M1)- Al^{3+}(Tet-site).

Sinusoidal crystallization trajectories are also observed for both A-17 VLT and Luna 24 VLT pyroxenes (Fig. 1a,b). A rise in the activity of Ti in late-stage liquids due to fractional crystallization of plagioclase and Ti-poor pyroxene causes the upswing of all trajectories and leads to the crystallization of Ti-rich spinel and ilmenite, which preferentially take up Fe relative to Mn. The HT and L-24 trends are the most strongly sinusoidal, with the other suites having flatter trends. The linear fits are illustrated in Fig. 1c. The HT basalts have a relatively steep slope (0.022) and the other suites have more typical lunar slopes of ~0.013.

These data imply that the activity of Ti in the basalts, their crystallization sequences, and the nature of the M1 site in pyroxene result in minor variations in the Mn/Fe of lunar pyroxene. This does not, however, reduce the usefulness of Mn/Fe in pyroxene as an indicator of planetary heritage. The mantle sources for all of these magmas must have had nearly identical Mn/Fe, suggesting that the Moon-wide primordial melting and differentiation event had little effect on this ratio in silicates. Increasing Ti activity should increase melt polymerization, and as Ti^{4+} abundances increase, $^{[IV]}Ti^{4+}$ and $^{[IV]}Fe^{2+}$ change to $^{[VI]}Ti^{4+}$ and $^{[VI]}Fe^{2+}$ in the melt structure [14]. The role of melt structure due to changes in the Ti content does not,

however, appear to be significant. The limited data available for Mn partitioning in silicates (e.g., [15]) show no correlation with melt structure.
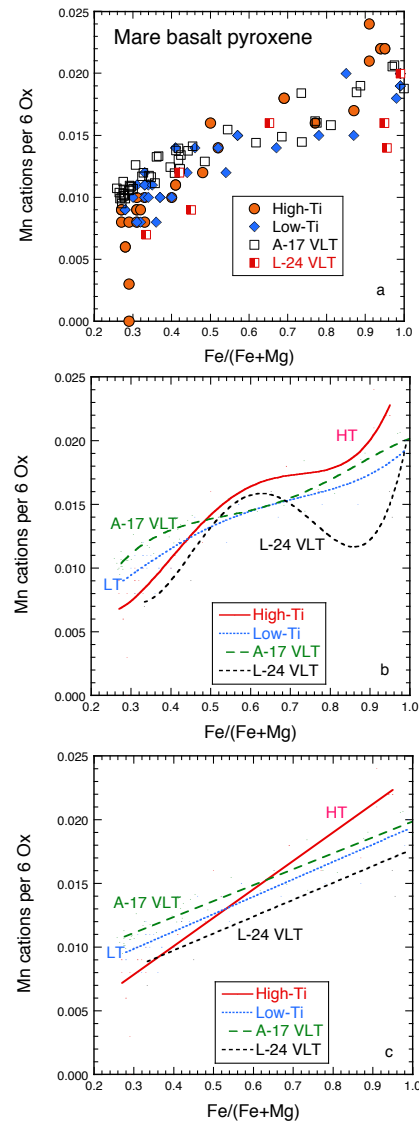
References: [1] Papike J. et al. (2003) *Am. Min., 88,* 469. [2] Papike J. et al. (2017) *Am. Min.,102,* 1759. [3] Mittlefehldt D. et al. (1998) *Revs. Mineral. 36,* 4-1. [4] Jolliff B. et al. (2000) *JGR, 105(E2)*, 4197. [5] Wadhwa M. (2008) *Revs. Mineral., 68,* 493. [6] Simon S. & Sutton S. (2017) *M&PS, 52,* 2015. [7] Papike J. et al. (2005) *Am. Min., 90,* 277. [8] Papike J. et al. (1976) *RGSP, 14*, 475. [9] Papike J. et al. (1998) *Revs. Mineral., 36,* 5-1. [10] Vaniman D. & Papike J. (1977) *GRL, 4,* 497. [11] Coish R. & Taylor L. (1978) *Mare Crisium* vol., 403. [12] Wentworth S. et al. (1979) *Proc. 10th LPSC*, 207. [13] Papike J. (1998) *Revs. Mineral. 36,* 7-1. [14] Vander Kaaden K. et al. (2015) *GCA, 149,* 1. [15] Longhi J. et al. (1978) *GCA, 42,* 1545.